Electronic Supplementary Information (ESI) for Chemical Communications

ATP dephosphorylation can be either enhanced or inhibited by pH-controlled interaction with a dendrimer molecule

Carla Bazzicalupi,[a] Antonio Bianchi,[a]* Claudia Giorgi,[a] Matteo Savastano[a] and Francisco Morales-Lara[b]

[a] Department of Chemistry "Ugo Schiff", University of Florence, Via della Lastruccia 3, 50019, Sesto Fiorentino, Italy. E-mail: antonio.bianchi@unifi.it
[b]Department of Inorganic Chemistry, University of Granada, 18071 Granada, Spain

Summary

Experimental procedures

Materials. Ligand L2 was synthesised as previously described.[1]

Potentiometric measurements

All pH-metric measurements (pH = -log [H^+]) employed for the determination of equilibrium constants were carried out in 0.1 M NMe_4Cl solutions at 298.1±0.1 K, by using the equipment and the methodology that has been already described.[2] The combined Hamilton glass electrode (LIQ-GLASS 238000/08) was calibrated as a hydrogen concentration probe by titrating known amounts of HCl with CO_2-free NMe_4OH solutions and determining the equivalent point by Gran's method[3] which allows one to determine the standard potential E^o and the ionic product of water (pK_w = 13.83(1) at 298.10.1 K in 0.1 M NMe_4Cl). At least three measurements were performed for each system in the pH ranges 2.5-11. In all experiments the ligand concentration [L] was about 1×10^{-3} M while, in anion binding experiments, the anion concentration [A] was varied in the range [L] ≤ [A] ≤ 3[L]. The computer program HYPERQUAD[4] was used to calculate the equilibrium constants from e.m.f. data.

1) S. H. Lee, D.-J. Kim, C.-C. Chang, S. S. Hah and J. Suh, *Bull. Korean Chem. Soc.*, 1998, **19**, 1270.

2) C. Bazzicalupi, A. Bianchi, C. Giorgi, P. Gratteri, P. Mariani and B. Valtancoli, *Inorg. Chem.*, 2013, **52**, 2125

3) (a) G. Gran, *Analyst* (London), 1952, **77**, 661; (b) *F. J.* Rossotti and H. Rossotti, *J. Chem. Educ.*, 1965, **42**, 375.

4) P. Gans, A. Sabatini and A. Vacca, *Talanta*, 1996, **43**, 1739.

^{1}H and ^{31}P NMR measurements

^{31}P (161 MHz) in D_2O solutions at different pH's were recorded at 298 K on a Bruker-Advance III 400 MHz spectrometer. Small amounts of 0.01 M NaOD and DCl were used to adjust the solutions pD. Complexation-induced ^{31}P chemical shifts (CIS, ppm) were measured as $(\delta_{OBS} - \delta)100/\%_{cplx}$ where δ_{OBS} is the chemical shift of a signal measured in D_2O solutions of ATP and L2 in a 1:1 molar ratio (both 10^{-2} M), δ is the chemical shift of the signal of ATP, under the same conditions, in the absence of L2 and $\%_{cplx}$ is the percentage of complex species present in solution under the condition used to record the spectrum. The pH was calculated from the measured pD value by using the relationship pH = pD – 0.40.[5]

The kinetics of ATP dephosphorylation were determined by keeping 0.01 M solutions of ATP and 0.001 M of L2 at pH 3 and 9 at 70 °C for increasing times. The reaction mixtures were rapidly

quenched to room temperature before recording the ^{31}P NMR spectra (Fig. S3). The signal of the P_β atom of ATP was used to quantify the amount of ATP that undergoes cleavage with time, showing that the dephosphorylation reaction proceeds though a first order kinetic according to the equation $\ln([ATP]/[ATP]_0) = -kt$, where [ATP] and $[ATP]_0$ are the concentration of ATP at t and t = 0 times, respectively (Figure S5). To avoid inhibition by reaction products, only the initial part of the ATP dephosphorylation process was followed. The experiments were repeated twice.

5) A. K. Covington, M. Paabo, R. A. Robinson and R. G. Bates, *Anal. Chem.*, 1968, **40**, 700.

Modelling calculations

Molecular modelling investigations on the adducts $[H_9L(ATP)]^{5+}$ and $[H_{15}L(H_2ATP)]^{13+}$ were performed by means of the empirical force field method AMBER3 as implemented in the Hyperchem 7.51 package,[6] using an implicit simulation of aqueous environment ($\varepsilon = 4r$) and atomic charged evaluated at the semiempirical level of theory (PM3).[7] Potential energy surface of all the systems has been explored by means of simulated annealing (T = 600 K, equilibration time = 10 ps, run time = 10 ps and cooling time = 10 ps, time step = 1.0 fs). For each studied system, 80 conformations have been sampled and those featured by an energy falling in the range of 3 kcal/mol from the minimum have been manually clusterized. The localization of acidic protons in the adducts was derived from the ligand protonation sequence deduced by means of ^1H NMR measurements (Fig. S6).

6) Hyperchem release 7.51 for Windows MM System, Hypercube, Inc., Gainesville, FL, 2002

7) (a) J. J. P. Stewart, *J. Comput. Chem.*, 1989, **10**, 209; (b) J. J. P. Stewart, *J. Comput. Chem.* 1989, **10**, 221.

Notes on ligand protonation and complex stability constants

In the first ten ligand protonation stages, it was not possible to distinguish single protonation processes, but only equilibria for the binding of couples of protons (two by two) were differentiated (Table S1). This phenomenon can be rationalized by considering that the protonation sites are identical and are located far apart from each other. In such a case, neither the nature of the groups undergoing protonation, nor the electrostatic repulsion within the pair of generated ammonium groups can separate the two protonation processes that, consequently, appear as a single protonation equilibrium involving two protons.

A similar phenomenon was also found for the anion binding processes (Tables S2-S7). For this reason, for several complexation equilibria, it was not possible to dissect the overall equilibrium constants (β values) determined for anion complexation ($L + nH^+ + A^{m-} = [H_nLA]^{(n-m)+}$) into equilibrium constants for the interaction between individual ligand and anion species ($H_iL^{i+} + H_{(n-i)}A^{(n-i-m)+} = [(H_iL)(H_{(n-i)}A)]^{(n-m)+}$). When it was possible, the location of protons in the complexes was assumed to be regulated by the basicity of the interacting species in agreement with previous studies.[8]

8) (a) *Anion Coordination Chemistry* (Eds.: K. Bowman-James, A. Bianchi, E. Garcia-España) Wiley-VCH, New York, **2012**; (b) J. L. Sessler, P. A. Gale and W.S. Cho, *Anion Receptor Chemistry* (Monographs in Supramolecular Chemistry); Series Ed.: J. F. Stoddart, RSC Publishing, Cambridge, **2006**; (c) E. Garcia-España, P. Díaz, J. M. Llinares and A. Bianchi, *Coord. Chem. Rev.*, 2006, **250**, 2952; (d) P. Mateus, N. Bernier and R. Delgado, *Coord. Chem. Rev.*, 2010, **254**, 1726; (e) C. Bazzicalupi, A. Bencini, A. Bianchi, M. Cecchi, B. Escuder, V. Fusi, E. Garcia-España, C. Giorgi, S. V. Luis, G. Maccagni, V. Marcelino, P. Paoletti and B. Valtancoli, *J. Am. Chem. Soc.*, 1999, **121**, 6807; (f) A. Bianchi, M. Micheloni and P. Paoletti, *Inorg. Chim. Acta*, 1988, **151**, 269; (g) A. Andrés, J. Aragó, A. Bencini, A. Bianchi, A. Domenech, V. Fusi, E. García-España, P. Paoletti and J. A. Ramírez, *Inorg. Chem.*, 1993, **32**, 3418.

Table S1. Protonation constants of ligand L2. (L) 0.10 M Me_4NCl, 298.1 ± 0.1 K.

	log*K*
$L + 2H^+ = H_2L^{2+}$	23.53(6)[a]
$H_2L^{2+} + 2H^+ = H_4L^{4+}$	20.90(6)
$H_4L^{4+} + 2H^+ = H_6L^{6+}$	19.40(6)
$H_6L^{6+} + 2H^+ = H_8L^{8+}$	18.69(6)
$H_8L^{8+} + 2H^+ = H_{10}L^{10+}$	17.60(6)
$H_{10}L^{10+} + H^+ = H_{11}L^{11+}$	8.32(4)
$H_{11}L^{11+} + H^+ = H_{12}L^{12+}$	8.33(4)
$H_{12}L^{12+} + H^+ = H_{13}L^{13+}$	8.01(4)
$H_{13}L^{13+} + H^+ = H_{14}L^{14+}$	6.81(5)
$H_{14}L^{14+} + H^+ = H_{15}L^{15+}$	5.72(4)
$H_{15}L^{15+} + H^+ = H_{16}L^{16+}$	5.46(4)
$H_{16}L^{16+} + H^+ = H_{17}L^{17+}$	3.76(5)
$H_{17}L^{17+} + H^+ = H_{18}L^{18+}$	2.27(6)

[a] Values in parentheses are standard deviation on the last significant figures.

Table S2. Stability constants of the complexes formed by L2 (L) with ATP. 0.10 M Me_4NCl, 298.1 ± 0.1 K.

	log*K*
$L + 2H^+ + ATP^{4-} = [H_2L(ATP)]^{2-}$	27.74(3) [a]
$L + 3H^+ + ATP^{4-} = [H_3L(ATP)]^-$	37.98(3)
$L + 5H^+ + ATP^{4-} = [H_5L(ATP)]^+$	58.09(3)
$L + 7H^+ + ATP^{4-} = [H_7L(ATP)]^{3+}$	77.42(3)
$L + 9H^+ + ATP^{4-} = [H_9L(ATP)]^{5+}$	96.11(2)
$L + 11H^+ + ATP^{4-} = [H_{11}L(ATP)]^{7+}$	113.84(2)
$L + 12H^+ + ATP^{4-} = [H_{12}L(ATP)]^{8+}$	121.89(4)
$L + 13H^+ + ATP^{4-} = [H_{13}L(ATP)]^{9+}$	130.23(2)
$L + 14H^+ + ATP^{4-} = [H_{14}L(ATP)]^{10+}$	137.37(2)
$L + 15H^+ + ATP^{4-} = [H_{15}L(ATP)]^{11+}$	143.92(2)
$L + 16H^+ + ATP^{4-} = [H_{16}L(ATP)]^{12+}$	149.63(2)
$L + 17H^+ + ATP^{4-} = [H_{17}L(ATP)]^{13+}$	154.16(2)
$L + 18H^+ + ATP^{4-} = [H_{18}L(ATP)]^{14+}$	157.62(2)
$H_{11}L^{11+} + ATP^{4-} = [H_{11}L(ATP)]^{7+}$	5.40(5)
$H_{12}L^{12+} + ATP^{4-} = [H_{12}L(ATP)]^{8+}$	5.12(5)
$H_{13}L^{13+} + ATP^{4-} = [H_{13}L(ATP)]^{9+}$	5.45(5)
$H_{14}L^{14+} + ATP^{4-} = [H_{14}L(ATP)]^{10+}$	5.78(4)
$H_{14}L^{14+} + HATP^{3-} = [H_{14}L(HATP)]^{11+}$	5.56(4)
$H_{15}L^{15+} + HATP^{3-} = [H_{15}L(HATP)]^{12+}$	5.55(4)
$H_{15}L^{15+} + H_2ATP^{2-} = [H_{15}L(H_2ATP)]^{13+}$	5.09(4)
$H_{16}L^{16+} + H_2ATP^{2-} = [H_{16}L(H_2ATP)]^{14+}$	4.19(4)

[a] Values in parentheses are standard deviation on the last significant figures.

Table S3. Stability constants of the complexes formed by L2 (L) with ADP. 0.10 M Me_4NCl, 298.1 ± 0.1 K.

	log*K*
$L + 2H^+ + ADP^{3-} = [H_2L(ADP)]^-$	30.68(3) [a]
$L + 3H^+ + ADP^{3-} = [H_3L(ADP)]^+$	41.21(3)
$L + 5H^+ + ADP^{3-} = [H_5L(ADP)]^{3+}$	61.25(3)
$L + 7H^+ + ADP^{3-} = [H_7L(ADP)]^{5+}$	80.08(3)
$L + 9H^+ + ADP^{3-} = [H_9L(ADP)]^{7+}$	98.33(3)
$L + 11H^+ + ADP^{3-} = [H_{11}L(ADP)]^{7+}$	115.53(3)
$L + 12H^+ + ADP^{3-} = [H_{12}L(ADP)]^{9+}$	123.57(3)
$L + 13H^+ + ADP^{3-} = [H_{13}L(ADP)]^{10+}$	131.42(3)
$L + 14H^+ + ADP^{3-} = [H_{14}L(ADP)]^{11+}$	138.12(3)
$L + 15H^+ + ADP^{3-} = [H_{15}L(ADP)]^{12+}$	144.23(2)
$L + 16H^+ + ADP^{3-} = [H_{16}L(ADP)]^{10+}$	149.55(2)
$L + 17H^+ + ADP^{3-} = [H_{17}L(ADP)]^{11+}$	153.94(2)
$L + 18H^+ + ADP^{3-} = [H_{18}L(ADP)]^{12+}$	157.51(2)
$H_{11}L^{11+} + ADP^{3-} = [H_{11}L(ADP)]^{8+}$	7.09(5)
$H_{12}L^{12+} + ADP^{3-} = [H_{12}L(ADP)]^{9+}$	6.80(5)
$H_{13}L^{13+} + ADP^{3-} = [H_{13}L(ADP)]^{10+}$	6.64(5)
$H_{14}L^{14+} + ADP^{3-} = [H_{14}L(ADP)]^{11+}$	6.53(4)
$H_{14}L^{14+} + HADP^{2-} = [H_{14}L(HADP)]^{12+}$	6.39(4)
$H_{15}L^{15+} + HADP^{2-} = [H_{15}L(HADP)]^{13+}$	6.00(5)
$H_{16}L^{16+} + HADP^{2-} = [H_{16}L(HADP)]^{14+}$	4.93(5)
$H_{17}L^{17+} + HADP^{2-} = [H_{17}L(HADP)]^{15+}$	4.74(5)

[a] Values in parentheses are standard deviation on the last significant figures.

Table S4. Stability constants of the complexes formed by L2 (L) with AMP. 0.10 M Me_4NCl, 298.1 ± 0.1 K.

	log*K*
$L + 2H^+ + AMP^{2-} = [H_2L(AMP)]^-$	27.87(4) [a]
$L + 3H^+ + AMP^{2-} = [H_3L(AMP)]^+$	38.74(3)
$L + 5H^+ + AMP^{2-} = [H_5L(AMP)]^{3+}$	58.92(3)
$L + 7H^+ + AMP^{2-} = [H_7L(AMP)]^{5+}$	77.87(3)
$L + 9H^+ + AMP^{2-} = [H_9L(AMP)]^{7+}$	96.06(3)
$L + 11H^+ + AMP^{2-} = [H_{11}L(AMP)]^{9+}$	113.25/3)
$L + 12H^+ + AMP^{2-} = [H_{12}L(AMP)]^{10+}$	121.11(5)
$L + 13H^+ + AMP^{2-} = [H_{13}L(AMP)]^{11+}$	129.22(3)
$L + 14H^+ + AMP^{2-} = [H_{14}L(AMP)]^{12+}$	135.93(4)
$L + 15H^+ + AMP^{2-} = [H_{15}L(AMP)]^{13+}$	142.04(4)
$L + 16H^+ + AMP^{2-} = [H_{16}L(AMP)]^{14+}$	147.67(4)
$L + 17H^+ + AMP^{2-} = [H_{17}L(AMP)]^{15+}$	152.55(4)
$L + 18H^+ + AMP^{2-} = [H_{18}L(AMP)]^{16+}$	156.72(3)
$H_{11}L^{11+} + AMP^{2-} = [H_{11}L(AMP)]^{9+}$	4.81(5)
$H_{12}L^{12+} + AMP^{2-} = [H_{12}L(AMP)]^{10+}$	4.34(7)
$H_{13}L^{13+} + AMP^{2-} = [H_{13}L(AMP)]^{11+}$	4.44(5)
$H_{14}L^{14+} + AMP^{2-} = [H_{14}L(AMP)]^{12+}$	4.34(6)
$H_{14}L^{14+} + HAMP^- = [H_{14}L(HAMP)]^{13+}$	4.11(7)
$H_{15}L^{15+} + HAMP^- = [H_{15}L(HAMP)]^{14+}$	4.02(6)
$H_{16}L^{16+} + HAMP^- = [H_{16}L(HAMP)]^{15+}$	3.44(6)
$H_{17}L^{17+} + HAMP^- = [H_{17}L(HAMP)]^{16+}$	3.85(6)

[a] Values in parentheses are standard deviation on the last significant figures.

Table S5. Stability constants of the complexes formed by L2 (L) with PO_4^{3-}. 0.10 M Me_4NCl, 298.1 ± 0.1 K.

	log*K*
$L + 2H^+ + PO_4^{3-} = [H_2L(PO_4)]^-$	29.07(6) [a]
$L + 4H^+ + PO_4^{3-} = [H_4L(PO_4)]^+$	50.34(6)
$L + 6H^+ + PO_4^{3-} = [H_6L(PO_4)]^{3+}$	70.10 (6)
$L + 8H^+ + PO_4^{3-} = [H_8L(PO_4)]^{5+}$	88.89(6)
$L + 10H^+ + PO_4^{3-} = [H_{10}L(PO_4)]^{7+}$	106.94(6)
$L + 12H^+ + PO_4^{3-} = [H_{12}L(PO_4)]^{9+}$	123.93(8)
$L + 13H^+ + PO_4^{3-} = [H_{13}L(PO_4)]^{10+}$	132.02(7)
$L + 14H^+ + PO_4^{3-} = [H_{14}L(PO_4)]^{11+}$	139.86(8)
$L + 15H^+ + PO_4^{3-} = [H_{15}L(PO_4)]^{12+}$	146.93(7)
$H_{12}L^{12+} + HPO_4^{2-} = [H_{12}L(HPO_4)]^{10+}$	3.6(1)
$H_{13}L^{13+} + HPO_4^{2-} = [H_{13}L(HPO_4)]^{11+}$	3.4(1)
$H_{13}L^{13+} + H_2PO_4^- = [H_{13}L(HPO_4)]^{12+}$	3.7(1)

[a] Values in parentheses are standard deviation on the last significant figures.

Table S6. Stability constants of the complexes formed by L2 (L) with $P_2O_7^{4-}$. 0.10 M Me_4NCl, 298.1 ± 0.1 K.

	log*K*
$L + 2H^+ + P_2O_7^{4-} = [H_2L(P_2O_7)]^{2-}$	28.30(6) [a]
$L + 3H^+ + P_2O_7^{4-} = [H_3L(P_2O_7)]^{-}$	38.63(6)
$L + 5H^+ + P_2O_7^{4-} = [H_5L(P_2O_7)]^{+}$	59.03(6)
$L + 7H^+ + P_2O_7^{4-} = [H_7L(P_2O_7)]^{3+}$	78.42(5)
$L + 9H^+ + P_2O_7^{4-} = [H_9L(P_2O_7)]^{5+}$	97.26(5)
$L + 11H^+ + P_2O_7^{4-} = [H_{11}L(P_2O_7)]^{7+}$	114.93(6)
$L + 12H^+ + P_2O_7^{4-} = [H_{12}L(P_2O_7)]^{8+}$	123.12(8)
$L + 13H^+ + P_2O_7^{4-} = [H_{13}L(P_2O_7)]^{9+}$	131.54(6)
$L + 14H^+ + P_2O_7^{4-} = [H_{14}L(P_2O_7)]^{10+}$	139.19(6)
$L + 15H^+ + P_2O_7^{4-} = [H_{15}L(P_2O_7)]^{11+}$	146.17(5)
$L + 16H^+ + P_2O_7^{4-} = [H_{16}L(P_2O_7)]^{12+}$	152.42(4)
$L + 17H^+ + P_2O_7^{4-} = [H_{17}L(P_2O_7)]^{13+}$	157.72(4)
$L + 18H^+ + P_2O_7^{4-} = [H_{18}L(P_2O_7)]^{14+}$	162.24(3)
$H_{11}L^{11+} + HP_2O_7^{3-} = [H_{11}L(HP_2O_7)]^{8+}$	5.8(1)
$H_{12}L^{12+} + HP_2O_7^{3-} = [H_{12}L(HP_2O_7)]^{9+}$	5.87(8)
$H_{13}L^{13+} + HP_2O_7^{3-} = [H_{13}L(HP_2O_7)]^{10+}$	5.51(8)
$H_{14}L^{14+} + HP_2O_7^{3-} = [H_{14}L(HP_2O_7)]^{11+}$	5.68(8)
$H_{15}L^{15+} + HP_2O_7^{3-} = [H_{15}L(HP_2O_7)]^{12+}$	6.21(7)
$H_{14}L^{14+} + H_2P_2O_7^{2-} = [H_{14}L(H_2P_2O_7)]^{12+}$	5.64(7)
$H_{15}L^{15+} + H_2P_2O_7^{2-} = [H_{15}L(H_2P_2O_7)]^{13+}$	5.22(7)
$H_{16}L^{16+} + H_2P_2O_7^{2-} = [H_{16}L(H_2P_2O_7)]^{14+}$	4.28(7)

[a] Values in parentheses are standard deviation on the last significant figures.

Table S7. Stability constants of the complexes formed by L2 (L) with $P_3O_{10}^{5-}$. 0.10 M Me_4NCl, 298.1 ± 0.1 K.

	log*K*
$L + H^+ + P_3O_{10}^{5-} = [HL(P_3O_{10})]^{4-}$	16.98(7) [a]
$L + 3H^+ + P_3O_{10}^{5-} = [H_3L(P_3O_{10})]^{2-}$	38.57(8)
$L + 5H^+ + P_3O_{10}^{5-} = [H_5L(P_3O_{10})]$	58.89(8)
$L + 7H^+ + P_3O_{10}^{5-} = [H_7L(P_3O_{10})]^{2+}$	79.03(7)
$L + 9H^+ + P_3O_{10}^{5-} = [H_9L(P_3O_{10})]^{4+}$	98.10(6)
$L + 11H^+ + P_3O_{10}^{5-} = [H_{11}L(P_3O_{10})]^{6+}$	116.12(6)
$L + 12H^+ + P_3O_{10}^{5-} = [H_{12}L(P_3O_{10})]^{7+}$	124.22(7)
$L + 13H^+ + P_3O_{10}^{5-} = [H_{13}L(P_3O_{10})]^{8+}$	132.80(7)
$L + 14H^+ + P_3O_{10}^{5-} = [H_{14}L(P_3O_{10})]^{9+}$	140.34(6)
$L + 15H^+ + P_3O_{10}^{5-} = [H_{15}L(P_3O_{10})]^{10+}$	147.36(6)
$L + 16H^+ + P_3O_{10}^{5-} = [H_{16}L(P_3O_{10})]^{11+}$	153.39(6)
$L + 17H^+ + P_3O_{10}^{5-} = [H_{17}L(P_3O_{10})]^{12+}$	158.56(6)
$L + 18H^+ + P_3O_{10}^{5-} = [H_{18}L(P_3O_{10})]^{13+}$	162.45(6)
$L + 19H^+ + P_3O_{10}^{5-} = [H_{19}L(P_3O_{10})]^{14+}$	165.45(8)
$H_{11}L^{11+} + HP_3O_{10}^{4-} = [H_{12}L(HP_3O_{10})]^{7+}$	7.27(9)
$H_{12}L^{12+} + HP_3O_{10}^{4-} = [H_{12}L(HP_3O_{10})]^{8+}$	7.52(8)
$H_{13}L^{13+} + HP_3O_{10}^{4-} = [H_{13}L(HP_3O_{10})]^{9+}$	7.05(8)
$H_{14}L^{14+} + HP_3O_{10}^{4-} = [H_{14}L(HP_3O_{10})]^{10+}$	7.26(8)
$H_{15}L^{15+} + HP_3O_{10}^{4-} = [H_{15}L(HP_3O_{10})]^{11+}$	7.57(8)
$H_{15}L^{15+} + H_2P_3O_{10}^{3-} = [H_{15}L(H_2P_3O_{10})]^{12+}$	7.11(8)
$H_{16}L^{16+} + H_2P_3O_{10}^{3-} = [H_{15}L(H_2P_3O_{10})]^{13+}$	5.54(8)
$H_{17}L^{17+} + H_2P_3O_{10}^{3-} = [H_{17}L(H_2P_3O_{10})]^{14+}$	4.78(9)

[a] Values in parentheses are standard deviation on the last significant figures.

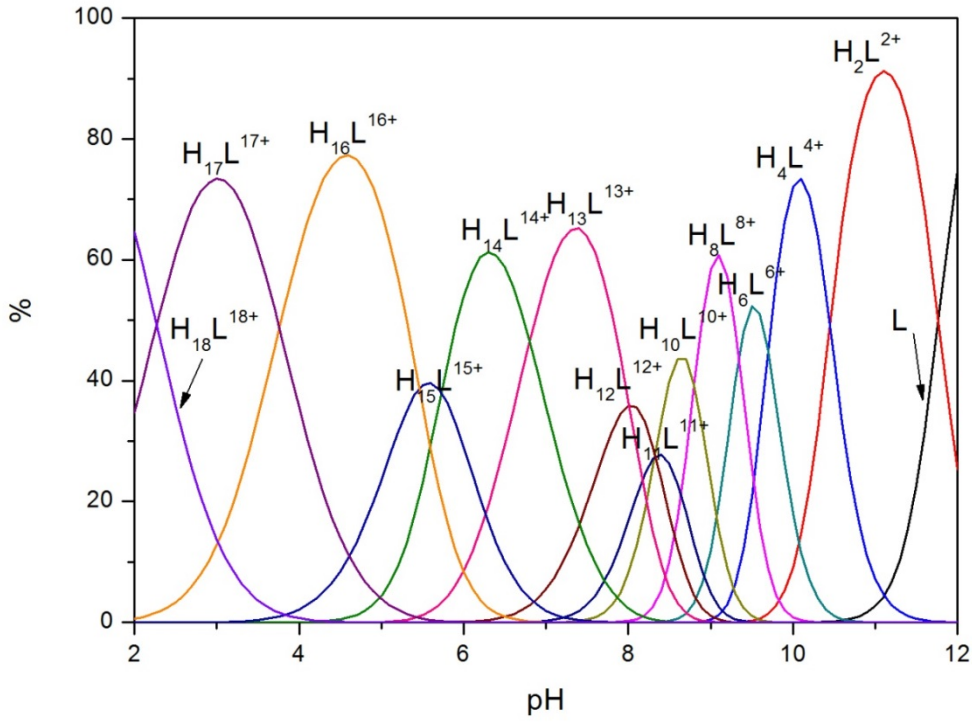

Figure S1. Distribution diagram of the protonated species formed by L2 (L) calculated by means of the equilibrium constants reported in Table S1. [L] = 0.001M.

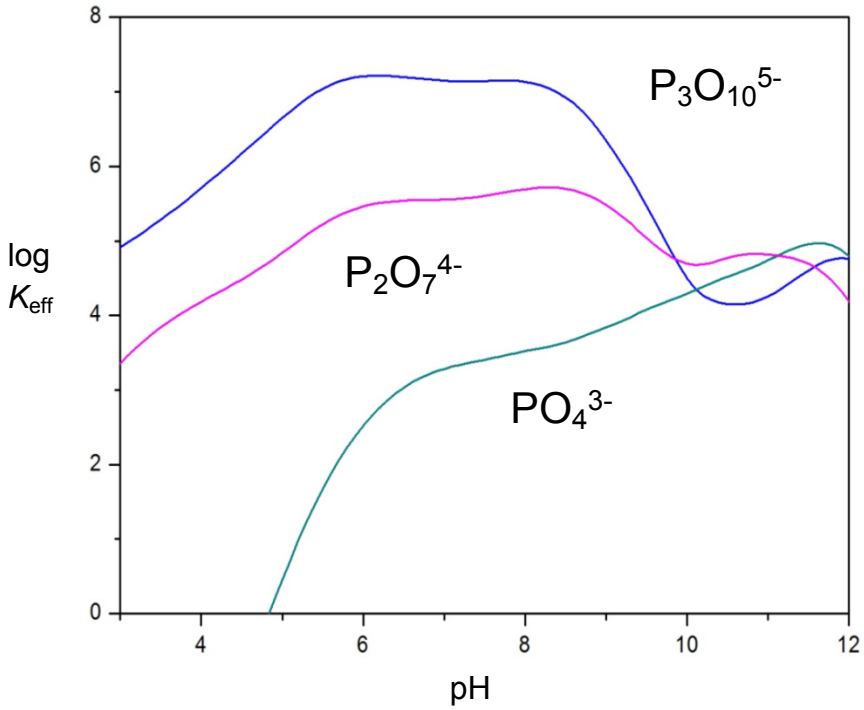

Figure S2. Logarithms of the effective stability constants (K_{eff}) for the interaction of L2 with PO_4^{3-}, $P_2O_7^{4-}$ and $P_3O_{10}^{5-}$ calculated as a function of pH.

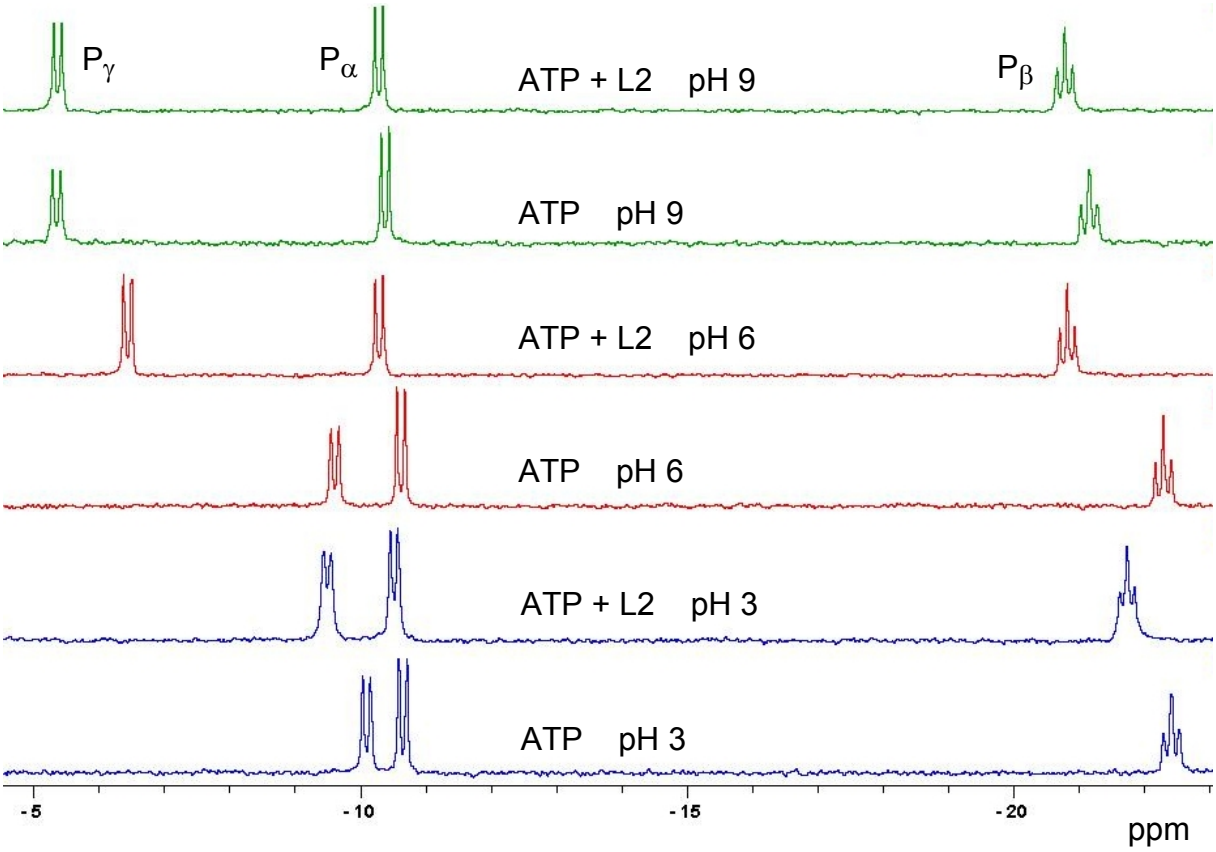

	Pγ	Pα	Pβ
pH 3			
ATP/L2 δ(ppm)	-9.51	-10.54	-21.75
CIS	0.72	0.14	0.84
pH 6			
ATP/L2 δ(ppm)	-6.45	-10.3	-20.84
CIS	3.21	0.33	1.48
pH 9			
ATP/L2 δ(ppm)	-5.38	-10.28	-20.8
CIS	0.04	0.09	0.37

Figure S3. ^{31}P NMR spectra recorded on D_2O solutions of ATP in the absence and in the presence of L2 at different pH's and corresponding coordination-induced shifts (CIS). [L2] = [ATP] = 0.01 M. CIS calculated for 100% complexation.

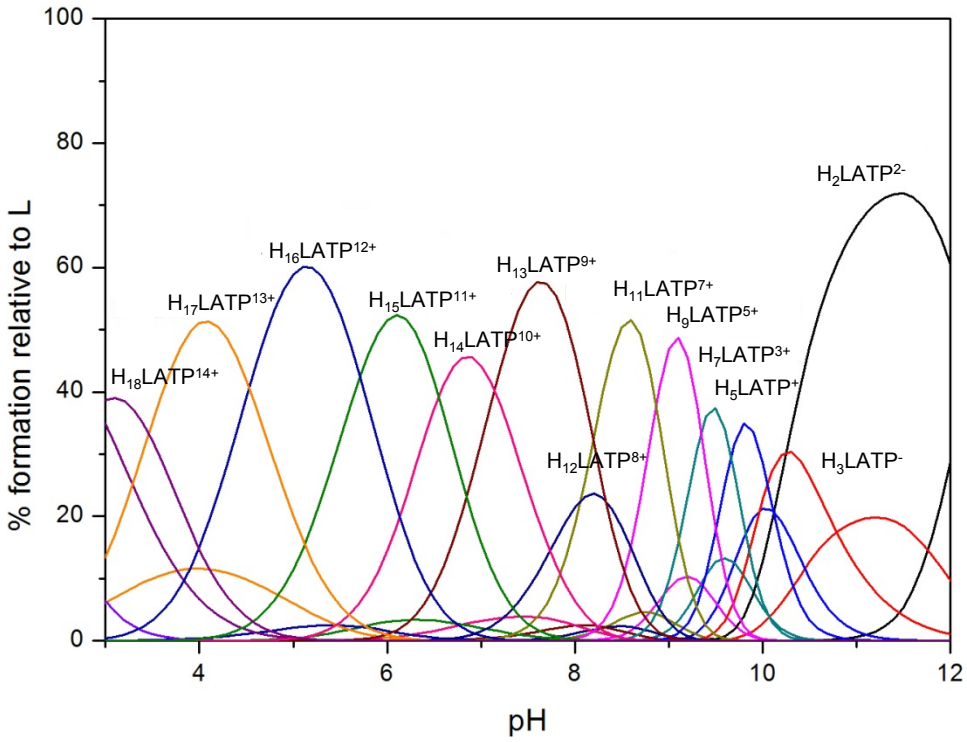

Figure S4. Distribution diagram of the species formed in the system ATP/L2 (L) calculated by means of the equilibrium constants reported in Table S2. [L] = [ATP] = 0.001M.

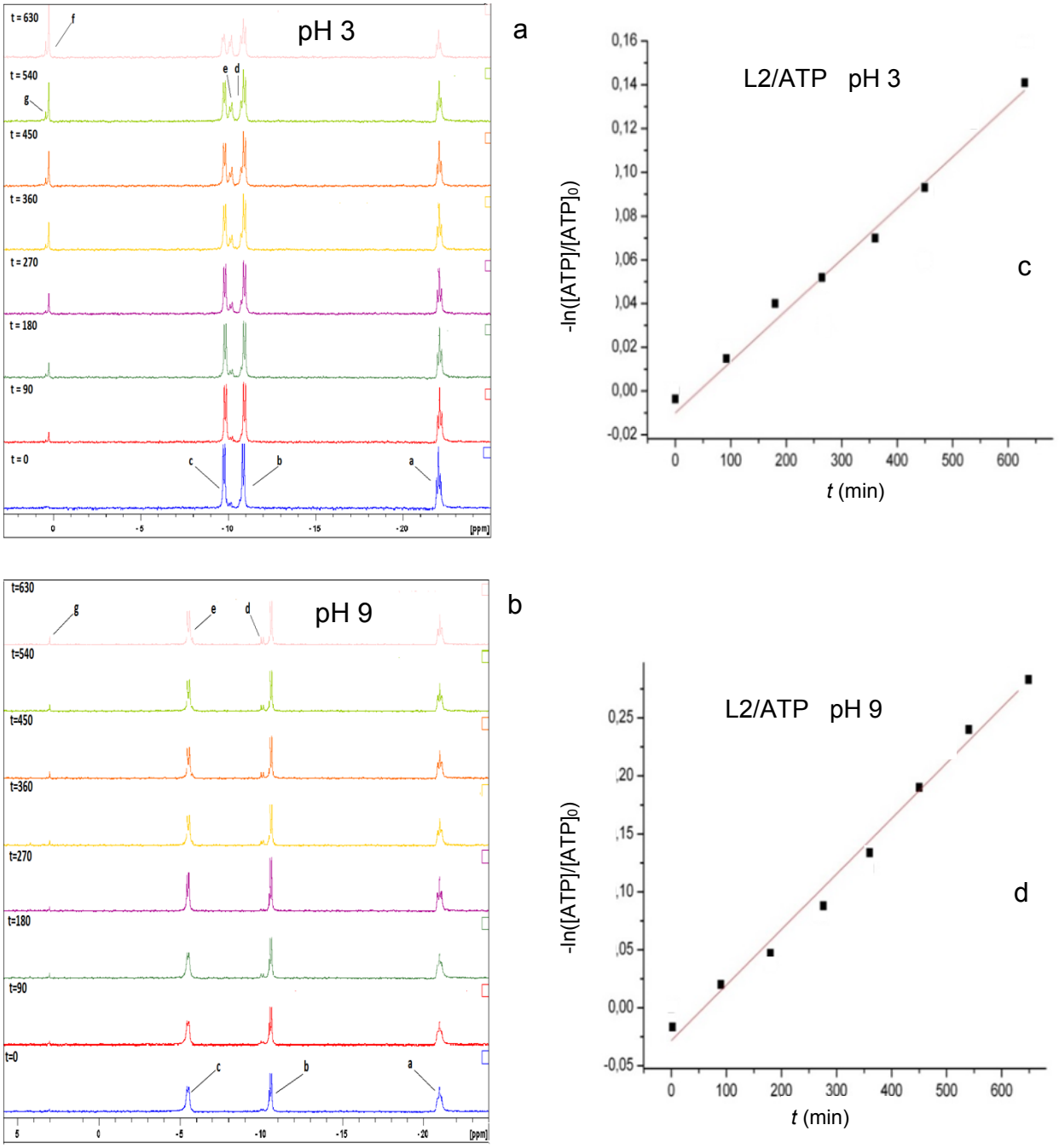

Figure S5. ^{31}P NMR spectra recorded on D_2O solutions of ATP in the presence of L2 at pH 3 (a) and 9 (b) after warming at 343.1 K for increasing times. Signal symbols: a, P_β of ATP; b, P_γ of ATP; c, P_α of ATP; d, P_α of ADP; e, P_β of ADP; f, P of AMP; g, inorganic phosphate. Corresponding plots of $-\ln([ATP]/[ATP]_0) = kt$, where [ATP] and $[ATP]_0$ are, respectively, the concentration of ATP at t and $t = 0$ times, at pH 3 (c) and 9 (d). [ATP] = 0.01 M, [L2] = 0.001 M.

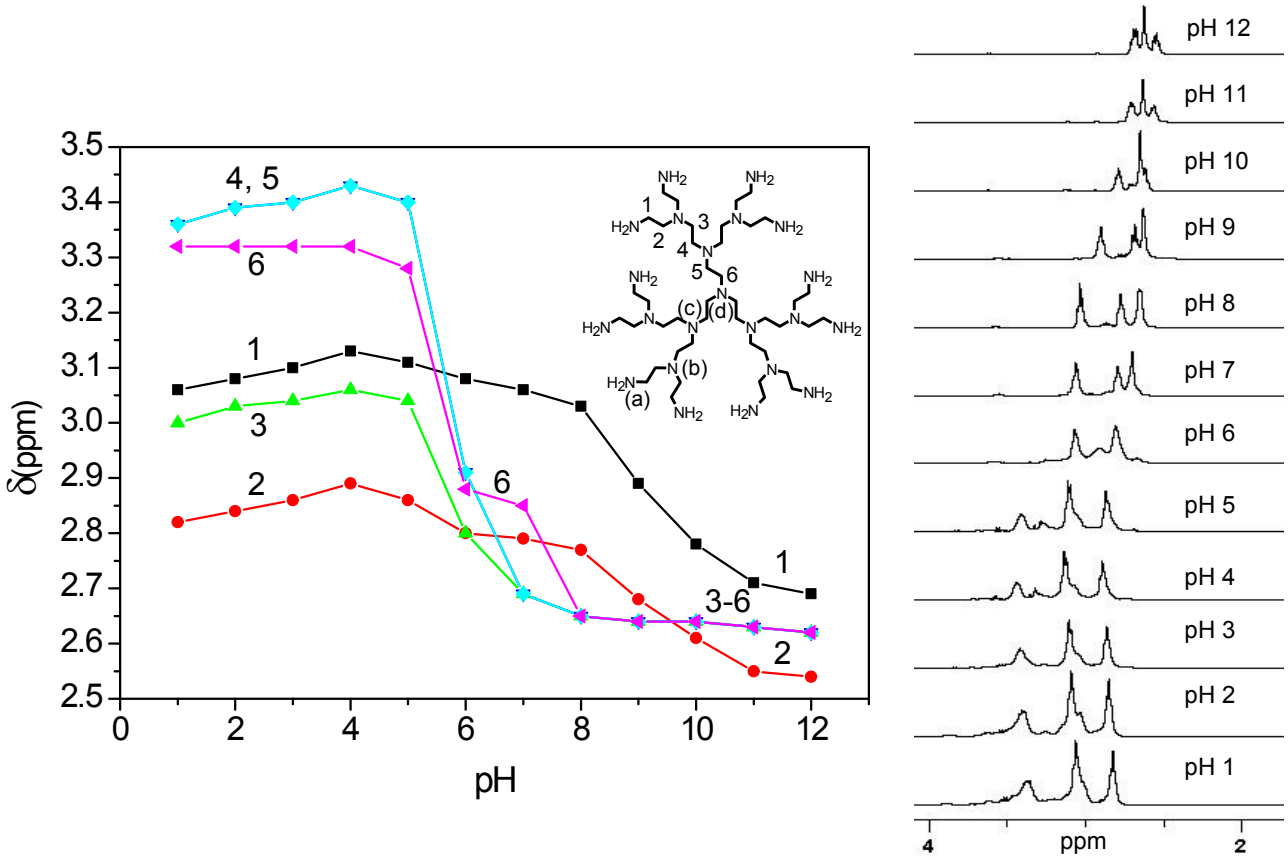

Figure S6. Variation of the ^{1}H NMR signals of L2 as a function of pH.

On the basis of the pH dependence of the ^{1}H NMR signals of L2 reported above and making reference to the species distribution diagram of Figure S1, we can infer which amine nitrogens or groups of amine nitrogens are involved in the successive protonation stages. The first 12 H^{+} ions bind the 12 primary N(a) atoms, which remain protonated in more acidic solutions. The 13rd proton binds the central tertiary N(d) nitrogen. In the two successive protonation stages, until the formation of the $H_{15}L2^{15+}$ species, three H^{+} ions are mostly involving the three N(c) nitrogens. Successive protonation causes a redistribution of protons over all tertiary amine groups.